PLAXIS

essential for geotechnical professionals

PLAXIS

# Site response analysis and liquefaction evaluation

2015

*Edited by:*

A. Laera
*PLAXIS bv, The Netherlands*

R.B.J. Brinkgreve
*Delft University of Technology & PLAXIS bv, The Netherlands*

## TABLE OF CONTENTS


**1 Introduction 5**
1.1 Liquefaction 6

**2 Example 17**
2.1 Simplified procedure 18

**3 Definition of the numerical model in PLAXIS 23**
3.1 Geometry model 23
3.2 Constitutive model 24
3.3 Definition of the loading condition 33
3.4 Mesh generation 34
3.5 Definition of the boundary conditions and of the calculation parameters 35
3.6 Results 37
3.7 Conclusions 40

**4 References 41**

# 1 INTRODUCTION

When an earthquake occurs, the seismic waves propagate from the source till the ground surface, causing ground shaking. The effects of an earthquake can be different, such as structural damages, landslides and soil liquefaction. In order to identify and mitigate the seismic hazards, appropriate earthquake engineering studies which involve different technical fields, such as geology, geotechnical and structural engineering, seismology are required.

One of the aspects that needs to be taken into consideration is the modification of the earthquake characteristics when seismic waves travel through the soil deposit, that acts as a filter.

In common practice and according to current regulations, there are three principal ways to evaluate the soil effects on the ground motion:

- The attenuation relationship approach
- The soil coefficient approach
- The site response analysis

The first two approaches are a simplification of the real soil distribution and their applicability is limited.

A site response analysis is commonly performed when soil conditions cannot be categorized into one of the standard site conditions or when the soil coefficient (as indicated in the current regulations) is not available (for instance, if the soil is classified as $S_1$ or $S_2$ according to EC8).

On the other hand, a site response analysis requires a deep and extended investigation of the soil deposit to identify the soil layer distribution and hydraulic conditions, and the mechanical properties of the soil. When possible, the investigation should be extended until the depth of a rock or rock-like formation. In situ and laboratory tests should be performed to evaluate index properties, stiffness and strength of the soil layers with regards to their behaviour under cyclic loading (Cross-hole and Down-hole in situ tests, among others, and cyclic triaxial, cyclic direct simple shear and resonant column laboratory tests).

A site response analysis allows for more elaborated results, i.e. the variation of the seismic waves in terms of amplitude, duration and frequency content at any depth of the soil deposit.

The ground response analysis of a soil deposit can be considered as a necessary preliminary study for the dynamic analysis of a structure, since its seismic response is influenced by the geological and geotechnical properties of the supporting soil. Due to its filter effect, the soil deposit modifies the seismic waves by amplifying the signal at some specific frequencies and damping it at some others. If the frequency at which the maximum amplification of the ground motion occurs is close to the natural frequency of the overlying structure, the building and the ground motion are in resonance with one another. This means that the system oscillates with very high amplitudes that can cause great damages in the building.

The site response analysis is performed in free field conditions, i.e. the motion that occurs in the soil layers at the depth of interest (for instance, at the foundation level in the

case of a building with shallow foundation) is determined by applying the selected earthquake at the bedrock, in the absence of any structure or excavation.

In order to perform a site response analysis, the following steps need to be accomplished:

- Definition of the geotechnical model of the soil deposit, in terms of soil layer distribution, water table depth, soil mechanical properties to describe its behaviour under static and cyclic loading;
- Definition of the seismic input motion, according to the specific site and the probabilistic study as reported in the current regulations (i.e. Eurocode 8, NTC 2008, etc.);
- Definition of the numerical model to perform the analysis.

Each of these steps involves a certain degree of uncertainty. The local soil stratigraphy, the material properties, the site topography, the ground water table depth and the characteristics of the earthquake (for example, duration, peak acceleration, frequency content, magnitude) have a high influence on the ground response and on the modelling strategy.

The selection of input ground motion time histories for site response analysis is regulated for each country. As for Europe, Eurocode 8 provide some guidelines in the selection and scaling of the accelerograms.

The definition of the geometry, boundary conditions and the selection of appropriate constitutive models to represent the soil behaviour are key features in the use of computer programs for site response analysis. Numerical methods are commonly used in engineering practice to perform site response analysis and the use of one-dimensional, bi-dimensional and tri-dimensional models is related to the specific site conditions.

One-dimensional analysis can be performed when the soil layers and the bedrock surface are horizontal and they extend to infinity, and the seismic waves coincide with shear waves propagating vertically from the underlying bedrock. This last assumption can be justified considering that the seismic waves, propagating from the earthquake source through the soil, are bent by successive refractions into a nearly vertical path (according to Snell's law of refraction).

When the above conditions are not verified, for example in the case of an irregular stratigraphy or a complex topography, it is advised to use 2D or 3D models.

## 1.1 LIQUEFACTION

The term liquefaction is used to describe a variety of phenomena that occurs in saturated cohesionless soils under undrained conditions. Under static and cyclic loading, dry cohesionless soils tend to densify. If these soils are saturated and the applied load acts in a short time, as in the case of an earthquake, the tendency to densify causes an increase in excess pore pressures that cannot be rapidly dissipated and consequently a decrease in the effective stresses occurs. When this happens, the soil behaves as a fluid.

This phenomenon can be explained considering that the shear resistance $\tau$ for cohesionless soils is given by Coulomb's formula:

$$\tau = \sigma'_{v0} tan\phi \tag{1.1}$$

where $\sigma'_{v0}$ is the initial effective stress and $\phi$ is the friction angle.

According to Terzaghi's formula, the effective stress is given by:

$$\sigma'_{v0} = \sigma_{v0} - u \tag{1.2}$$

where $\sigma_{v0}$ is the total vertical stress and $u$ is the pore pressure. When the excess pore pressures develop during an earthquake, the equation can be written as:

$$\sigma'_{v0} = \sigma_{v0} - (u + \Delta u) \tag{1.3}$$

which means that the effective stress state tends to decrease and, when it reaches zero, also the shear resistance is null. In order to evaluate the potential liquefaction hazard of a site, it is necessary to identify the predisposing and triggering factors for liquefaction.

The predisposing factors are the characteristics of the soil deposit such as particle size and shape, gradation, plasticity characteristics. The triggering factors depend on the earthquake magnitude, duration and peak ground acceleration.

To establish if liquefaction will occur in a specific site subjected to a selected earthquake semi-empirical procedures or dynamic methods can be used. The semi-empirical procedures consist in the evaluation of a safety factor as the ratio of the cyclic shear stress required to cause liquefaction and the equivalent cyclic shear stress induced by the earthquake. The dynamic method is based on a one-dimensional wave propagation analysis in terms of effective stresses, which gives the possibility to calculate the pore pressure ratio at any depth.

### 1.1.1 SEMI-EMPIRICAL PROCEDURES FOR TRIGGERING LIQUEFACTION

The semi-empirical procedure to evaluate liquefaction potential during earthquakes was introduced by Seed & Idriss (1971) and subsequently updated by Idriss & Boulanger (2014). It consists in the evaluation of a safety factor given by the ratio of the cyclic resistance ratio CRR, i.e. the capacity of the soil to resist liquefaction, and the cyclic stress ratio CSR, i.e. the equivalent cyclic shear stress induced by the earthquake.

$$FS = \frac{CRR}{CSR} \tag{1.4}$$

The threshold value of the safety factor can be different for different countries. According to Eurocode 8, liquefaction can occur when the safety factor is less than 1.25.

#### *Cyclic stress ratio*

The transformation of the earthquake induced loading into an equivalent series of uniform stress cycles is required, since the laboratory data from which liquefaction resistance can be estimated are usually obtained from tests in which the cyclic shear stresses have uniform amplitudes.

The cyclic stress ratio CSR, at a particular depth in a soil deposit, is expressed as:

$$CSR = \frac{\tau_a}{\sigma'_{v0}} = 0.65 \frac{\tau_{max}}{\sigma'_{v0}} \tag{1.5}$$

where $\tau_a$ is the average equivalent uniform shear stress induced by the earthquake,

assumed to have an amplitude of 65% of the peak cyclic shear stress.

Seed & Idriss (1971) have provided a simplified formula to calculate the uniform cyclic shear stress amplitude:

$$CSR = 0.65 \cdot \frac{a_{max}}{g} \cdot \frac{\sigma_{v0}}{\sigma'_{v0}} \cdot r_d \tag{1.6}$$

where $a_{max}$ is the peak horizontal acceleration at ground surface, $g$ is the acceleration of gravity, $\sigma_{v0}$ and $\sigma'_{v0}$ are the total and effective initial vertical stresses, respectively, and $r_d$ is a stress reduction factor dependent on the considered depth in the soil and earthquake magnitude. For routine practice and noncritical projects, the following equations may be used to estimate average values of $r_d$ (Idriss (1999)):

$$r_d = exp\,[\alpha(z) + \beta(z)M] \tag{1.7}$$

where

$$\alpha(z) = -1.012 - 1.126\ sin\left(\frac{z}{11.73} + 5.133\right) \tag{1.8}$$

$$\beta(z) = 0.106 + 0.118\ sin\left(\frac{z}{11.26} + 5.142\right) \tag{1.9}$$

where z is the depth below the ground surface, in meters, and M is the magnitude. The $r_d$ coefficient can also be calculated from the chart proposed by Idriss & Boulanger (2004) and Idriss & Boulanger (2008) in Figure 1.1

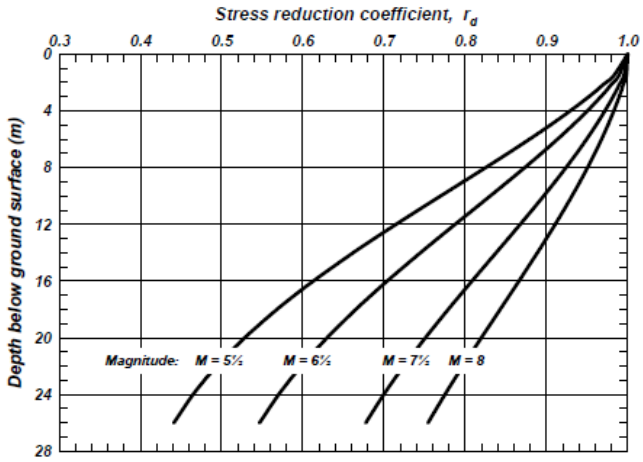


Figure 1.1 Values of $r_d$, calculated for M = 5.5, 6.5, 7.5 and 8 using equations derived by Idriss (1999), and used in the interpretations of liquefaction/no liquefaction case histories by Idriss & Boulanger (2004) and Idriss & Boulanger (2008).

Since all correlations in literature are based on earthquakes of magnitude 7.5, a magnitude scaling factor *MSF* has to be used to adjust the induced CSR during an earthquake of magnitude M. The overburden correction factor $K_\sigma$ accounts for the non linearity of the overburden pressure, since laboratory cyclic triaxial compression tests

show that the liquefaction resistance of a soil increases with increasing confining pressure but the resistance decreases with increased normal stress in a non linear way. The overburden correction factor allows to scale the CSR ratio for a reference effective stress of 1 atm (100 kPa).

The charts to determine the soil liquefaction resistance are based on the normalized CSR ratio, i.e. $CSR_{M=7.5|\sigma'_{v0}=1atm}$:

$$CSR_{M=7.5|\sigma'_{v0}=1atm} = \frac{CSR_M}{MSF \cdot K_\sigma} \tag{1.10}$$

where MSF is:

$$MSF = min\left(6.9\, exp\left(\frac{-M}{4}\right) - 0.058; 1.8\right) \tag{1.11}$$

and

$$K_\sigma = 1 - C_\sigma ln\left(\frac{\sigma'_{v0}}{p_a}\right) \leq 1.1 \tag{1.12}$$

The $K_\sigma$ relationship was developed by Boulanger, Kutter, Brandenberg, Singh & Chang (2003), while the coefficient $C_\sigma$ depends on the in situ measurements and can be expressed in terms of the $(N_1)_{60,cs}$ or $q_{c1Ncs}$ values Idriss & Boulanger (2008) :

$$C_\sigma = \frac{1}{18.9 - 2.55\sqrt{(N_1)_{60,cs}}} \leq 0.3 \tag{1.13}$$

$$C_\sigma = \frac{1}{37.3 - 8.27 \cdot (q_{c1Ncs})^{0.264}} \leq 0.3 \tag{1.14}$$

where $(N_1)_{60,cs}$ and $q_{c1Ncs}$ are the normalized penetration resistance for clean sands based on SPT and CPT tests, respectively, as it will be explained in the next subsection. In order to define the equivalent cyclic shear stress induced by the earthquake, magnitude and peak horizontal ground acceleration have to be estimated. These factors characterize duration and intensity of the ground motion, respectively, but their determination represents a critical aspect in liquefaction analysis.

The latest guidelines published in the report from the NCEER/NSF workshop Youd et al (2001) suggest three different methods to estimate $a_{max}$:

- Empirical correlations of $a_{max}$ with earthquake magnitude, distance from the seismic source, local site conditions, in the case of sites on bedrock or stiff to moderately stiff soils. The selection of an appropriate attenuation relationship should be based on factors such as country, type of faulting and site conditions.
- Local site response analysis in the case of soft sites or other soil profiles that are not compatible with available attenuation relationship. It is suggested to use recorded accelerograms.
- Use of amplification ratios, as described by Idriss (1990) and Idriss (1991) and Seed, Dickenson, Rau, White & Mok (1994). In this way, bedrock outcrop motions are multiplied by an amplification ratio to estimate surface motion at the soil site. This method should be used carefully since the amplification ratios are influenced by the level of strain, the earthquake magnitude and the frequency content.

If $a_{max}$ is estimated through a site response analysis, the generation of excess pore pressure and the onset of liquefaction should be neglected. In this way, the resulting peak acceleration accounts for the site amplification but it is not influenced by the increase of excess pore pressure in the areas in which the soil may soften and the motion may be reduced.

As for the earthquake magnitude, the moment magnitude is the scale preferred for liquefaction resistance. The main uncertainties are represented by the difficulty of assigning a unique value to the earthquake magnitude in a specific area, considering that the dynamic response of a soil deposit is a function of different seismic events with different magnitude and different distances between the seismic source and the site of interest.

### *Cyclic resistance ratio*

The liquefaction resistance CRR is generally evaluated from in situ tests. According to the various methods, CRR is derived by charts where CRR is plotted as a function of normalized SPT blow counts, CPT tip resistance or shear wave velocity vs, as shown in Figure 1.2 and Figure 1.3. The CRR curve separates the area that identifies the occurrence of liquefaction from the area in which no liquefaction will happen. The curves are based on normalized values of the liquefaction resistance to account for the earthquake magnitude and the effect of the confining stress.

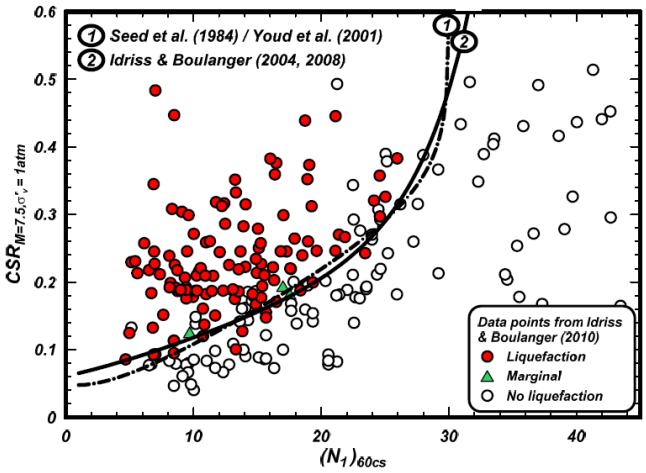


Figure 1.2 Examples of SPT-based liquefaction triggering curves for M = 7.5 and $\sigma'_v$ = 1 atm with a database of case histories processed with the Idriss-Boulanger (2008) procedure (Idriss & Boulanger (2008))

In order to use SPT blow count and CPT tip resistance to identify liquefaction potential in a soil, it is required to separate the effect of soil relative density ($D_R$) from the effective confining stress. For this reason, the normalized penetration resistance for SPT and CPT procedures are:

$$(N_1)_{60} = C_N \cdot (N)_{60} \tag{1.15}$$

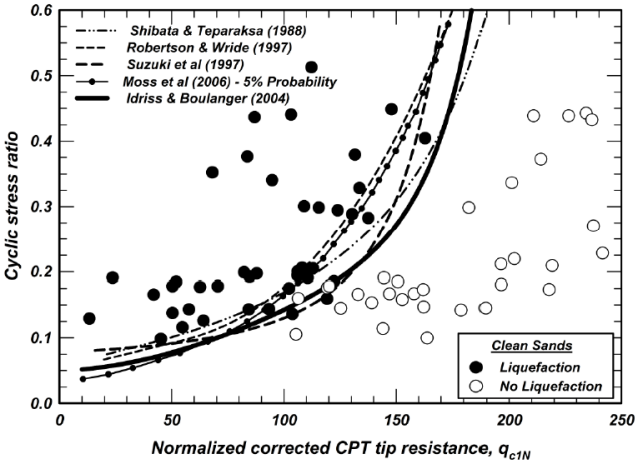


Figure 1.3 Examples of CPT-based liquefaction triggering curves for M = 7.5 and $\sigma'_v$ = 1 atm with an earlier database of clean sand liquefaction case histories processed with the Idriss-Boulanger (2008) procedure (Idriss & Boulanger (2008))

$$q_{c1N} = C_N \cdot \frac{q_c}{p_a} \tag{1.16}$$

where $C_N$ is an overburden correction factor, $(N)_{60}$ is the corrected SPT blow counts to account for the characteristics of the test, and $p_a$ is the atmospheric pressure (equal to 100 kPa if $q_c$ is expressed in kPa).

The value of $C_N$ can be calculated as:

$$C_N = \left( \frac{p_a}{\sigma'_{v0}} \right)^m \tag{1.17}$$

The exponent $m$ was considered equal to 0.5 in Lioa & Whitman(1986). Subsequently, new formulas are proposed Boulanger, Kutter, Brandenberg, Singh & Chang (2003); Idriss & Boulanger (2004)):

$$m = 0.784 - 0.521 \cdot D_R \tag{1.18}$$

$$m = 0.784 - 0.0768\sqrt{(N_1)_{60}} \tag{1.19}$$

$$m = 1.338 - 0.249 \cdot (q_{c1Ncs})^{0.264} \tag{1.20}$$

Both Eq. (1.19) and Eq. (1.20) require an iterative process of calculation.

The SPT blow count $N_{SPT}$ is affected by a number of procedural details (rod lengths, hammer energy, sampler details, borehole size). The normalized penetration resistance can be calculated as:

$$(N)_{60} = C_E \cdot C_R \cdot C_B \cdot C_S \cdot N_{SPT} \tag{1.21}$$

where $C_E$ is equal to $ER_m/60$, where $ER_m$ (in %) is the measured value of the delivered

energy as a percentage of the theoretical free-fall hammer energy, $C_R$ is a correction factor to account for different rod lengths, $C_B$ is a correction factor for nonstandard borehole diameters, $C_S$ is a correction factor that depends on the sampler, $N_{SPT}$ is calculated as $N_2 + N_3$, considering that $N_1$ $N_2$ and $N_3$ are the number of blows needed for the tube to penetrate each 15 cm.

Table 1.1 contains a list of the values of the different coefficients:

| Coefficient | Condition | Value |
|---|---|---|
| General | | |
| Borehole diameter, $C_B$ | 65 ÷ 115 mm (standard) | 1.00 |
| | 150 mm | 1.05 |
| | 200 mm | 1.15 |
| Rod length, $C_R$ | 3 ÷ 4 m | 0.75 |
| | 4 ÷ 6 m | 0.85 |
| | 6 ÷ 10 m | 0.95 |
| | 10 ÷ 30 m | 1.00 |
| | > 30 m | 1.00 |
| Type of sampler, $C_S$ | Standard | 1.00 |
| | Non standard | 1.1 ÷ 1.3 |

Table 1.1 Coefficients to calculate normalized $N_{SPT}$.

The liquefaction case histories suggest that the liquefaction triggering correlations shift to the left as the fines content (FC) increases, as has been reflected in recent CPT-based and SPT-based correlations (Figure 1.4 and Figure 1.5). These curves can be expressed using the following equations, based on the equivalent clean sand value of $(N_1)_{60}$, indicated as $(N_1)_{60,cs}$:

$$(N_1)_{60,cs} = (N_1)_{60} + \Delta(N_1)_{60} \tag{1.22}$$

where

$$\Delta(N_1)_{60} = exp\left[1.63 + \frac{9.7}{FC} - \left(\frac{15.7}{FC}\right)^2\right] \tag{1.23}$$

Then, the value of CRR for a magnitude M of 7.5 and an effective vertical stress of 100 kPa can be calculated as:

$$CRR = exp\left[\frac{(N_1)_{60,cs}}{14.1} + \left(\frac{(N_1)_{60,cs}}{126}\right)^2 - \left(\frac{(N_1)_{60,cs}}{23.6}\right)^3 + \left(\frac{(N_1)_{60,cs}}{25.4}\right)^4 - 2.8\right] \tag{1.24}$$

Idriss & Boulanger (2004) observed that the reliability of any liquefaction evaluation depends directly on the quality of the site characterization, and it is often the synthesis of findings from several different procedures that provides the most insight and confidence in making final decisions. For this reason, the practice of using a number of in situ testing

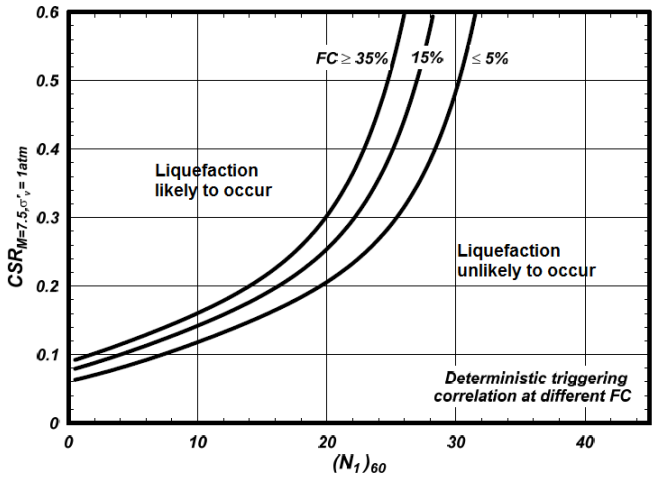


Figure 1.4 Deterministic SPT-based triggering correlation for clean sands and for cohesionless soils having various values of fine content, FC (Idriss and Boulanger 2014).

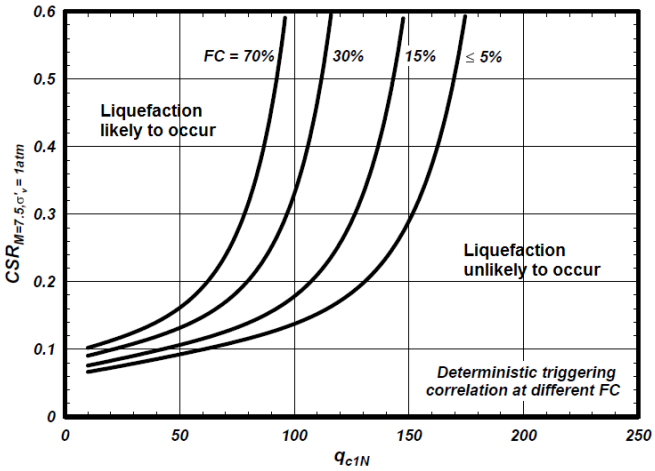


Figure 1.5 Revised deterministic CPT-based triggering correlation for clean sands and for cohesionless soils having various values of fine content, FC (Idriss and Boulanger 2014).

methods should continue to be the basis for standard practice, and the allure of relying on a single approach (e.g. CPT-only procedures) should be avoided.

### 1.1.2 EUROCODE 8

Eurocode 8 provides the standard for the design of structures for earthquake resistance. Part 5 of Eurocode 8 is devoted to foundations, retaining structures and geotechnical aspects, and it contains requirements regarding specific analysis in potentially liquefiable soils (par. 4.1.4).

According to EC8 (2004): "An evaluation of the liquefaction susceptibility shall be made when the foundation soils include extended layers or thick lenses of loose sand, with or

without silt/clay fines, beneath the water table level, and when the water table level is close to the ground surface. This evaluation shall be performed for the free-field site conditions (ground surface elevation, water table elevation) prevailing during the lifetime of the structure." And: "Investigations required for this purpose shall as a minimum include the execution of either in situ Standard Penetration Tests (SPT) or Cone Penetration Tests (CPT), as well as the determination of grain size distribution curves in the laboratory."

Among others, this document states that the risk of liquefaction may be neglected when the following condition is met, $\alpha$ S < 0.15 and at least, one of the following conditions is fulfilled:

- the sands have a clay content greater than 20% with a plasticity index PI> 10;
- the sands have a silt content greater than 35% and an SPT blow count, normalized for overburden effects and the energy ratio, of $(N_1)_{60}$ > 20;
- the sands are clean, with an SPT blow count, normalized for overburden effects and the energy ratio, of $(N_1)_{60}$ > 30.

where $\alpha$ is the ratio of the design ground acceleration on type A ground, $a_g$, to the acceleration of gravity, g, and S is the soil factor. Therefore, EC8 provides a limit for the acceleration at the site surface equal or larger than 0.15 g for the occurrence of liquefaction.

The soil factor assumes different values for different soil classes. The site should be classified according to the value of the shear wave velocity $v_{s,30}$, i.e. the shear wave velocity calculated through a weighting procedure of the contribution of the layers included in the first 30 m from the ground surface. The soil classes are 7. Class A corresponds to a rock or rock-like formation, while class B, C, D and E correspond to soil characterized by a stiffness from moderate to low. Special ground types are $S_1$ and $S_2$ for which special studies for the definition of the seismic action are required (Figure 1.6). The soil coefficient $S$ for each ground type to be used in a country may be found in its National Annex.

The design ground acceleration on type A ground, $a_g$ may be derived from zonation maps specific of each country, as in its National Annex. Usually, the peak acceleration is different according to the return period considered. In the case a site response analysis is required, a proper number of compatible accelerograms has to be selected. Depending on the nature of the application and on the information actually available, the description of the seismic action may be made by using artificial accelerograms and recorded or simulated accelerograms.

In verifications of dynamic stability involving calculations of permanent ground deformations the excitation should preferably consist of accelerograms recorded on soil sites in real earthquakes, as they possess realistic low frequency content and proper time correlation between horizontal and vertical components of motion.

The suite of accelerograms should observe the following rules:

- a minimum of 3 accelerograms should be used (common practice suggests to use a set of 7 time history acceleration graphs);
- the mean of the zero period spectral response acceleration values (calculated from the individual time histories) should not be smaller than the value of $a_g \cdot S$ for the

| Ground type | Description of stratigraphic profile | Parameters | | |
|---|---|---|---|---|
| | | $v_{s,30}$ (m/s) | $N_{SPT}$ (blows/30cm) | $c_u$ (kPa) |
| A | Rock or other rock-like geological formation, including at most 5 m of weaker material at the surface. | > 800 | – | – |
| B | Deposits of very dense sand, gravel, or very stiff clay, at least several tens of metres in thickness, characterised by a gradual increase of mechanical properties with depth. | 360 – 800 | > 50 | > 250 |
| C | Deep deposits of dense or medium-dense sand, gravel or stiff clay with thickness from several tens to many hundreds of metres. | 180 – 360 | 15 - 50 | 70 - 250 |
| D | Deposits of loose-to-medium cohesionless soil (with or without some soft cohesive layers), or of predominantly soft-to-firm cohesive soil. | < 180 | < 15 | < 70 |
| E | A soil profile consisting of a surface alluvium layer with $v_s$ values of type C or D and thickness varying between about 5 m and 20 m, underlain by stiffer material with $v_s$ > 800 m/s. | | | |
| $S_1$ | Deposits consisting, or containing a layer at least 10 m thick, of soft clays/silts with a high plasticity index (PI > 40) and high water content | < 100 (indicative) | – | 10 - 20 |
| $S_2$ | Deposits of liquefiable soils, of sensitive clays, or any other soil profile not included in types A – E or $S_1$ | | | |

Figure 1.6 Soil classification. EC8, 2004

selected site.

- in the range of periods between $0.2 \cdot T_1$ and $2 \cdot T_1$, where $T_1$ is the fundamental period of the structure in the direction where the accelerogram will be applied; no value of the mean 5% damping elastic spectrum, calculated from all time histories, should be less than 90% of the corresponding value of the 5% damping elastic response spectrum.

The output represents the average result of ground response analyses performed for the same site by applying the selected seismic input signals.

## 2 EXAMPLE

In this example, it is supposed that the in situ characterization leads to the following soil stratigraphy: a clay layer extends from the ground surface to 5 m depth and is followed by 10 m of loose or medium loose sand for which 5 SPT measurements are performed every 2 meters (Table 2.1). The in situ tests are performed until a depth of 40 m, where a rock-like formation has been identified. The material from 15 to 40 m is characterized by clay. It is supposed that the shear wave velocity varies with depth as in Figure 2.1, with a minimum vs of 113 m/s at the top of the clay layer. The water table is supposed to be coincident with the ground surface level, so that the whole soil deposit is totally saturated.

| Depth (m) | $N_{SPT}$ |
|---|---|
| 5 | 5 |
| 7 | 7 |
| 9 | 6 |
| 11 | 8 |
| 13 | 10 |

Table 2.1 SPT blow counts in the sand layer

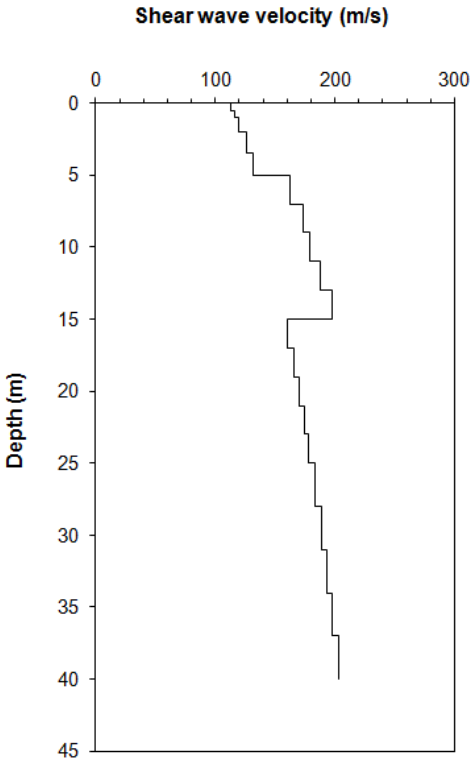


Figure 2.1 Shear wave velocity profile

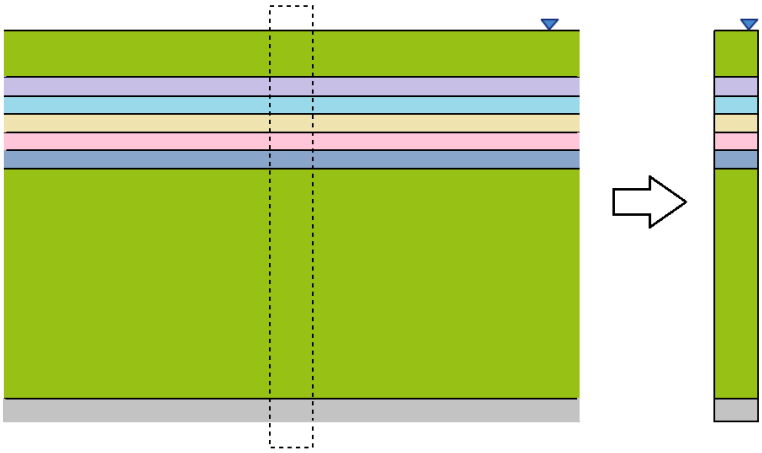

Figure 2.2 Soil stratigraphy

The layers and the bedrock surface are assumed to be horizontal and to extend to infinity. The ground surface is horizontal so no topographic effects need to be taken into consideration. A one-dimensional wave propagation can be performed (Figure 2.2). The target acceleration-time history is scaled to a peak ground acceleration of 0.3 g, recorded at the outcrop of a rock formation and characterized by a magnitude Mw of 6.9 and a duration of 40 seconds (Figure 2.3).

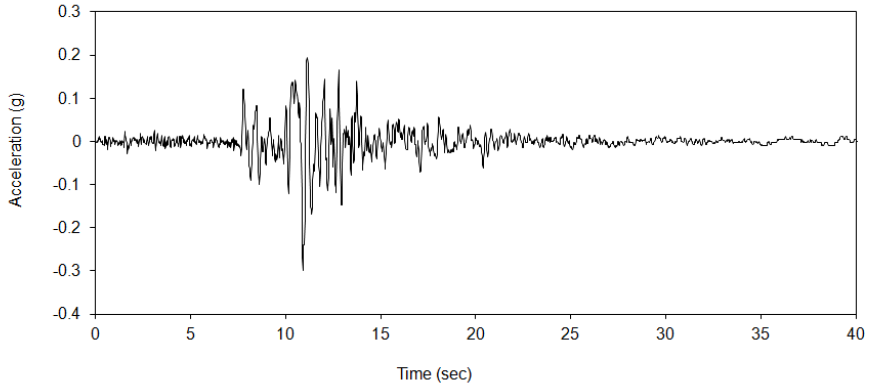


Figure 2.3 Target acceleration

## 2.1 SIMPLIFIED PROCEDURE

According to the simplified procedure, it is requested to calculate the liquefaction resistance CRR from in situ tests.

To calculate the corrected penetration resistance $(N)_{60}$, it is supposed that a standard borehole diameter and a standard sampler are used, so that the coefficient $C_B$ and $C_S$ are equal to 1. The rod length is supposed to be between 10 and 30 m, so that also the

coefficient $C_S$ is equal to 1. As for the hammer energy, it is supposed that the SPT procedure delivers about 72 % of the theoretical free fall energy to the sampler, i.e.:

$$C_E = \frac{E_m}{0.6 \cdot E_{eff}} = \frac{0.72 \cdot E_{eff}}{0.6 \cdot E_{eff}} = 1.2 \tag{2.1}$$

The corrected penetration resistance $(N)_{60}$ at each depth is then (Table 2.2):

| Depth (m) | $(N)_{60}$ |
|---|---|
| 5 | 6 |
| 7 | 8.4 |
| 9 | 7.2 |
| 11 | 9.6 |
| 13 | 12 |

Table 2.2 Corrected penetration resistance $(N)_{60}$ in the sand layer

The normalized penetration resistance depends on the value of $C_N$, that is a function of the effective vertical stress and the relative density of the sand. The value of $C_N$ is calculated according to the 3 different procedures available in literature which lead to very slightly different results. Table 2.3 illustrates the different values of the coefficient $C_N$ using all the three available procedure, for the first sand layer (depth = 5 m, $N_{SPT}$ = 5, $D_R$ = 40%)

| m | $C_N$ | $(N_1)_{60}$ |
|---|---|---|
| 0.5 | 1.348 | 8.09 |
| 0.565 | 1.415 | 8.49 |
| 0.560 | 1.398 | 8.39 |

Table 2.3 Corrected penetration resistance $(N_1)_{60}$ in the first sand layer

For all the 5 sand layers, the following normalized penetration resistance $(N_1)_{60}$ are calculated and supposing that the fine content is less than 5 % in the sand layers, the liquefaction resistance of each layer can be determined from the chart (Table 2.4, Figure 2.4):

| Depth (m) | $(N_1)_{60}$ | CRR |
|---|---|---|
| 5 | 8.09 | 0.11 |
| 7 | 9.97 | 0.12 |
| 9 | 7.72 | 0.10 |
| 11 | 9.46 | 0.11 |
| 13 | 11 | 0.13 |

Table 2.4 Normalized penetration resistance $(N_1)_{60}$ and liquefaction resistance CRR in the sand layers

The liquefaction resistance CRR of each sand layer has to be compared with the cyclic stress ratio induced by the earthquake CSR. Eq. (1.5) requires to calculate the peak

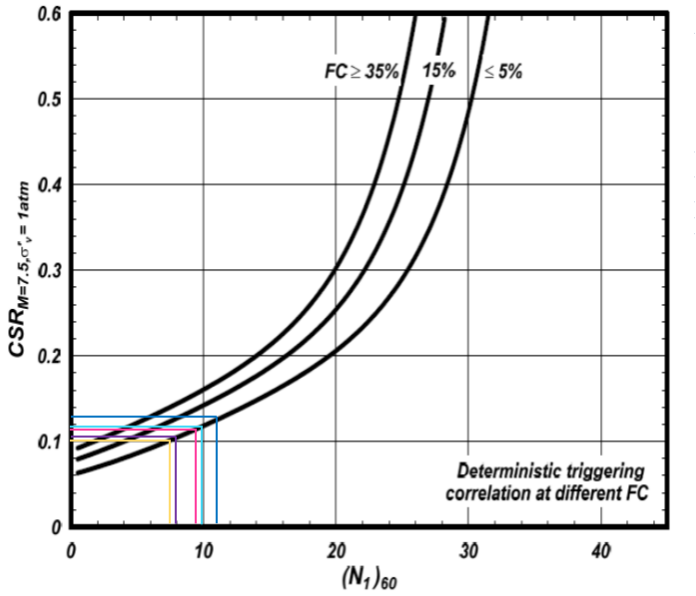


Figure 2.4 Calculated values of the liquefaction resistance (Idriss & Boulanger (2014))

ground acceleration $a_{max}$ and the $r_d$ coefficient, which is a function of the magnitude of the earthquake and the depth of the soil layer.

The peak ground acceleration can be calculated with different procedures. As it is explained in Eurocode 8, in case of liquefiable soils, the corresponding site class is $S_2$ for which no soil coefficients are available. This means that, in principle, the simplified procedure that allows to calculate the maximum acceleration for that site as the product between the peak acceleration relative to a rock formation and the soil coefficient is not applicable. In this case, it is suggested to perform a site response analysis selecting an appropriate set of accelerograms.

For this example, the calculation has been made considering only one accelerogram, but the same procedure has to be repeated for all the other selected accelerograms. The process to select the accelerograms is not explained in detail here.

The time history acceleration considered for this example is the following, recorded at the outcrop of a rock-like formation and scaled to a peak acceleration of 0.3 g. The magnitude is 6.9. A site response analysis is performed with EERA leading to a peak ground acceleration of 0.457 g, which accounts for the soil effects. The $r_d$ coefficient is calculated at each depth, taking into account the magnitude of the seismic events. As explained in Section 1.1.1, the CSR values need to be normalized by the magnitude scaling factor *MSF* and the overburden correction factor $K_\sigma$, so that, the following values are calculated and the factor of safety can be evaluated (Section 1.1.1) (Table 2.5)

The same analysis is now performed using PLAXIS. The characteristics of the model in terms of geometry, material models and boundary conditions will be explained in the next section.

| Depth (m) | $CSR_{M=7.5\|\sigma'_{v0}=1atm}$ | FS |
|---|---|---|
| 5 | 0.435 | 0.24 |
| 7 | 0.444 | 0.27 |
| 9 | 0.446 | 0.23 |
| 11 | 0.440 | 0.26 |
| 13 | 0.431 | 0.29 |

Table 2.5 Cyclic stress ratio and factor of safety according to the simplified procedure.

# 3 DEFINITION OF THE NUMERICAL MODEL IN PLAXIS

In order to perform a liquefaction analysis in PLAXIS 2D, it is necessary to:

- Define a representative geometry model
- Select appropriate constitutive models to reproduce the actual behaviour of the soil
- Apply the input motion
- Generate the mesh according to the minimum required length of the element
- Choose the boundary conditions as a function of the input motion and the characteristics of the site
- Set the appropriate calculation parameter

In this example, a one-dimensional wave propagation analysis is performed.

## 3.1 GEOMETRY MODEL

The wave propagation can be studied as a simplified one-dimensional problem in the case the soil layers and the surface are horizontal and they extend to infinity. The seismic waves coincide with shear waves propagating in the vertical direction. This condition can be modeled considering a soil column where the horizontal dimension is chosen in the order of the required element length, considering the applied seismic load and the characteristics of the soil, while the vertical dimension coincides with the soil deposit thickness.

In PLAXIS, 8 soil layers are specified considering a clay layer above and below the sand deposit, that is discretized into 5 layers according to the available $N_{SPT}$ measurements. The bottom layer is modeled as a rock formation, with the same characteristics of the outcropping rock where the signal is recorded. Refer Section 3.5 for more information.

The following soil stratigraphy can be specified in PLAXIS:

- from 41 to 36 m (clay layer)
- from 36 to 34 m (sand layer 1)
- from 34 to 32 m (sand layer 2)
- from 32 to 30 m (sand layer 3)
- from 30 to 28 m (sand layer 4)
- from 28 to 26 m (sand layer 5)
- from 26 to 1 m (clay layer)
- from 1 to 0 m (rock formation) (refer Section 3.5)

The water table is considered coincident with the ground surface level, i.e. the head parameter is set to 41 m.

## 3.2 CONSTITUTIVE MODEL

The selection of appropriate soil constitutive models in engineering problems is an important aspect of the modelling process. It should be noted that any soil model, even the most complex, is a simplification of the real soil behaviour and it involves a certain number of limitations. The constitutive model should be chosen according to the characteristics of the problem and the features that are considered to be determinant in the overall behaviour.

On one hand, constitutive models with a reduced number of parameters are quite easy to calibrate but more assumptions on soil behaviour are made and cannot be controlled by the user. On the other hand, complex constitutive models give the possibility to model more features of the soil behaviour, but they require an adequate knowledge of the model parameters and an extensive soil characterization to perform an appropriate calibration.

It has been chosen to model the clay layers with the Generalized Hardening Soil model, while the sand layers have been modeled using the UBC3D-PLM model, i.e. the 3D UBCSAND model for liquefaction analysis (Tsegaye (2010)) subsequently updated by Petalas & Galavi (2013). The Generalized Hardending Soil model can be obtained from PLAXIS Sales department (http://kb.plaxis.nl/models/udsm-generalized-hardening-soil-model).

### 3.2.1 CALIBRATION OF THE GENERALIZED HARDENING SOIL MODEL

The Generalized Hardening Soil model (GHS) is a user-defined soil model that can be applied in different geotechnical problems. It is a more modular version of the original Hardening Soil model with small strain stiffness (HSsmall), since it allows to use different configurations for the stress and strain dependency, and to select the appropriate yielding functions. For the four features described below it is possible to select the appropriate option using the corresponding number from 0 to 3 (or 4 in the case of the "plasticity model" feature).

These features are expressed by the following material parameters:

- Stress Dependent Stiffness, i.e. the soil stiffness is constant during the calculation based on the reference stiffness (0), or its value is constant during the phase but based on the stresses at the beginning of the calculation phase (1), or it is updated for every calculation step based on the chosen stress dependency formula (2)
- Strain Dependent Stiffness, that can be either not active (0) as in the Hardening Soil model, or active (1) as for the HS small model
- Stress Dependency formula, for which 3 options are available among : stress dependency based on $\sigma_3$ and strength parameters as in the HS small model(0), stress dependency based on $\sigma_3$ and preconsolidation pressure (1), and stress dependency based on mean effective stress and preconsolidation pressure (2);
- Plasticiy model, i.e. the user can activate only Mohr Coulomb failure criterion (0), or shear hardening and Mohr Coulomb failure criterion (1), or cap hardening and Mohr Coulomb failure criterion (2), or all the previous conditions (cap and shear hardening + Mohr Coulomb failure criterion) as in the HS small (4).

For this example, the following combination has been used:

- Stress Dependent Stiffness = 1 (To model the variation of the soil stiffness with

depth, based on the stresses at the beginning of the calculation phase)

- Strain Dependent Stiffness = 1 (To reproduce the stiffness decay due to the strain level related to the applied loads)
- Stress Dependency formula = 0 (To express the dependency of the soil stiffness on the minimum principal stress and the strength properties, such as cohesion and friction angle, according to a power rule (Eq. (3.1)))
- Plasticiy model = 1 (To activate only the Mohr Coulomb failure criterion so that the soil damping depends on the amount of energy dissipated through the hysteric loop until failure is reached, and no additional damping due to plastic deformations (that may lead to an overestimation of the total damping) is accounted for)

A detailed explanation of the soil behaviour during the cyclic loading is explained below.

In general, the soil stiffness is characterized by non-linear behaviour, both stress and strain dependent, i.e., even in a homogeneous lithological soil deposit, the soil stiffness varies with depth and its value decays with the strain level induced by the loading. The maximum strain at which the soil behaviour can be considered purely elastic is very small (in the order of $1 \cdot 10^{-6}$). The soil stiffness associated with this strain range is indicated as initial stiffness and its value decays by increasing the strain amplitude according to the characteristic S-curve in the logarithmic scale (Modulus reduction curve) (Figure 3.1).

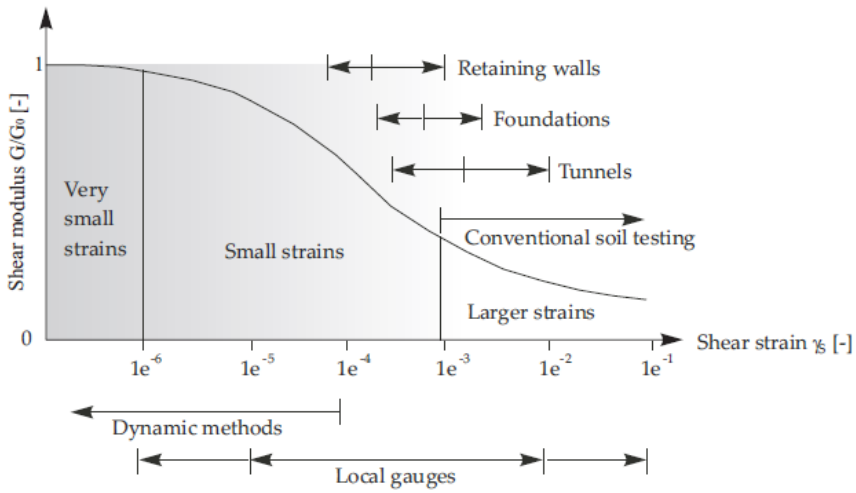


Figure 3.1 Stiffness-strain behaviour

In dynamic conditions, the soil is subjected to cyclic shear loading, showing not only a non linear but also a dissipative behaviour. The hysteretic loop generated during cyclic shear loading consists of a sequence of loading and unloading paths, because of the irreversible behaviour of the soil. In general, it has been observed that earthquakes induce a small strain level in the soil, that exhibits a high shear stiffness $G_0$, and that $G$ decreases while the amount of dissipated energy increases by increasing the magnitude of the shear strain $\gamma$. To account for these aspects of material behaviour, the Generalized Hardening Soil model, based on the HS small model and the Hardening Soil model, is used in this example. The Hardening Soil model already accounts for the stress dependency of the stiffness according to a power law expressed by the $m$ parameter.

Compared to the Hardening Soil model, the HS small model is extended by introducing two additional parameters that are kept also in the GHS model: the high stiffness at small strain level ($G_0$) and the shear strain at which $G$ has reduced to 70 % of the initial $G_0$ ($\gamma_{0.7}$).

The stress dependency is expressed by the following formula (option 0 for the Stress Dependency Formula):

$$G_0 = G_0^{ref} \left( \frac{c \cdot cos\varphi - \sigma'_3 \cdot sin\varphi}{c \cdot cos\varphi + p^{ref} \cdot sin\varphi} \right)^m \tag{3.1}$$

where the initial shear stiffness $G_0$ is a function of the effective stress, the strength parameters ($c$ and $\phi$) and the $m$ parameter which depends on the soil type (it generally varies between 0.5 and 1, according to the soil type). The typical hysteretic behaviour is shown in Figure 3.2. The initial tangent and secant stiffness of the initial loading curve coincide with the maximum shear stiffness $G_0$. By increasing the shear strain, the stiffness decays. When the load direction is inverted, the stiffness starts from the same $G_0$ and decreases until the next load reversal.

The stress-strain relationship is given by:

$$\tau = G_s \cdot \gamma \tag{3.2}$$

where $G_s$ represents the secant shear stiffness.

The strain-dependent secant shear modulus is expressed by:

$$G_s = \frac{G_0}{1 + 0.385 \frac{\gamma}{\gamma_{0.7}}} \tag{3.3}$$

The local hysteretic damping ratio is described by the following formula:

$$\xi = \frac{E_D}{4\pi E_S} \tag{3.4}$$

where $E_D$ represents the dissipated energy, given by the area of the closed loop (yellow and green areas), and $E_S$ is the energy accumulated at the maximum shear strain $\gamma_C$ (green and blue areas). The damping ratio $\xi$ applies until the material behaviour remains elastic and the shear modulus decreases with the strain.

To calibrate the parameters that need to be entered in PLAXIS, it is suggested to refer to experimental data from site and laboratory tests performed in the chosen area. Considering the Eq. (3.1), it is possible to calibrate $G^{ref}$ and $m$ in order to have the best fitting. In this example, the parameters are chosen according to some considerations since no data are available. The decay of the shear modulus with strain is displayed in Figure 3.3. The green curve shows the ratio of the secant shear modulus over the initial shear stiffness $G_s/G_0$ and the orange curve shows the ratio of the tangent shear modulus over the initial shear stiffness $G_t/G_0$, which can be calculated from Eq. (3.2) by taking the derivative with respect to the shear strain. The $G_s/G_0$ curve is described in literature by Vucetic & Dorby (1991) according to different values of the plasticity index. In this example, the clay layer is characterized by a plasticity index PI of 50 % and the relative curve is displayed in blue. The value of $\gamma_{0.7}$ has to be chosen in order to have the

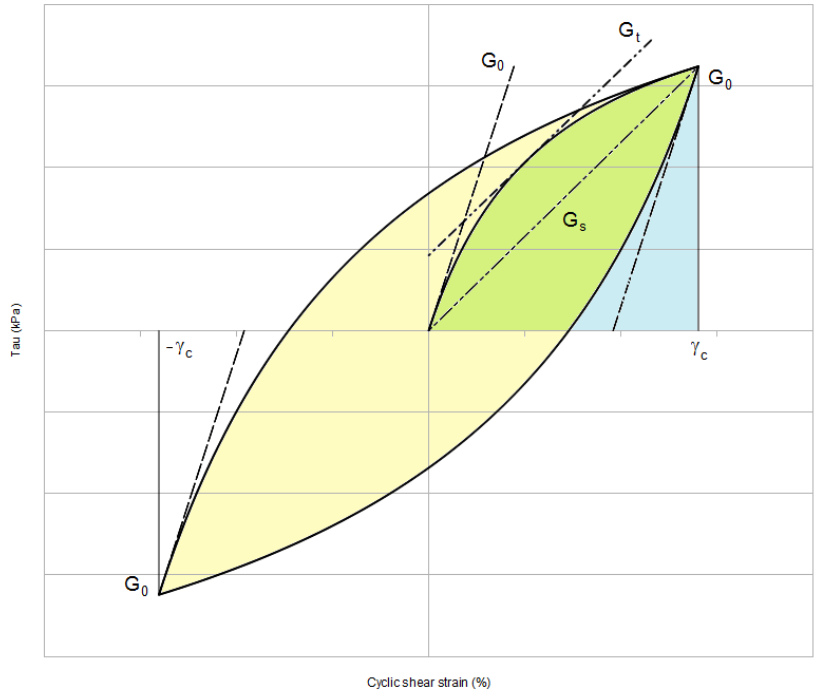


Figure 3.2 Hysteretic behaviour

best fitting between the calculated $G_s/G_0$ and the curve relative to the specific PI from Vucetic & Dorby (1991).

In the HS small model, the tangent shear modulus is bound by a lower limit, $G_{ur}$, to scale back to the original Hardening Soil model at higher strain levels. $G_{ur}$ is related to $E_{ur}$ and $\nu_{ur}$ according to the following expression:

$$G_{ur} = \frac{E_{ur}}{2(1+\nu_{ur})} \tag{3.5}$$

The shear strain that corresponds to the point in which the secant shear stiffness $G_t$ reaches the value of $G_{ur}$ represents the cut-off shear strain $\gamma_{cut-off}$, i.e. the limit above which the shear stiffness cannot decrease more than the reached $G_{ur}$ value.

$$\gamma_{cut-off} = \frac{\gamma_{0.7}}{0.385}\left(\sqrt{\frac{G_0}{G_{ur}}} - 1\right) \tag{3.6}$$

The initial shear stiffness at the reference pressure, $G_0^{ref}$, is taken equal to 48000 $kN/m^2$ in order to have a good approximation of the shear modulus variation with depth in the clay layer (Figure 3.4). Setting the ratio $G_0^{ref}$ over $G_{ur}^{ref}$ equal to 5 (which generally varies between 2.5 and 10 times going from hard to soft soils), the corresponding $G_{ur}^{ref}$ is taken equal to 9600 $kN/m^2$. According to Eq. (3.5), for $\nu_{ur}$ equal to 0.2, $E_{ur}^{ref}$ can be calculated, while $E_{50}^{ref}$ and $E_{oed}^{ref}$ are taken as 1/3 of $E_{ur}^{ref}$.

The damping ratio evolves as a function of the shear strain and it increases for larger

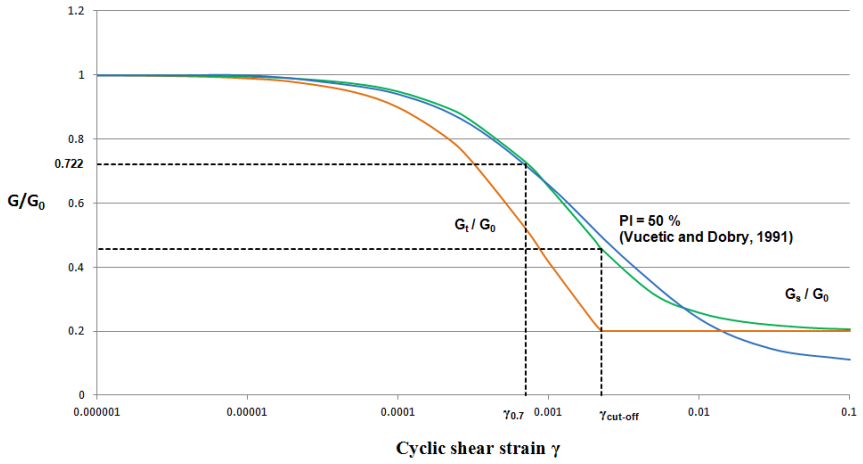


Figure 3.3 Modulus reduction curves

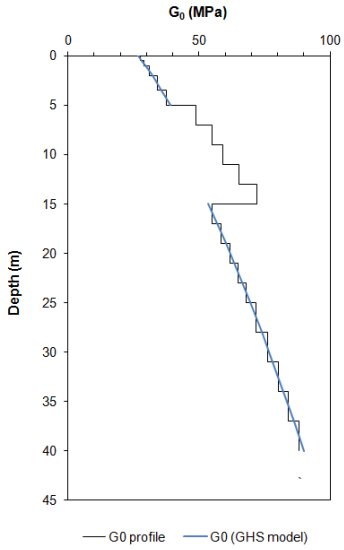


Figure 3.4 G profile

values of $\gamma$. In order to calibrate the value of $\gamma_{0.7}$, also the damping curve has to be taken into account. The Figure 3.5 represents the best fitting reached in this example, compared to the curve determined by Vucetic & Dorby (1991) for a clay characterized by PI equal to 50%. Also in this case, the cut-off shear strain represents the limit above which the damping ratio $\xi$ cannot increase further.

As for the drainage type, the Undrained A condition has been chosen. The whole soil deposit consists of a totally saturated cohesive soil. Considering that earthquakes act for a very short time, excess pore pressures are generated and cannot be dissipated during the seismic motion. The short term condition, i.e. undrained behaviour of the soil, has to be applied. In PLAXIS, the Undrained A condition allows to perform an undrained analysis by defining effective stiffness and effective strength parameters.

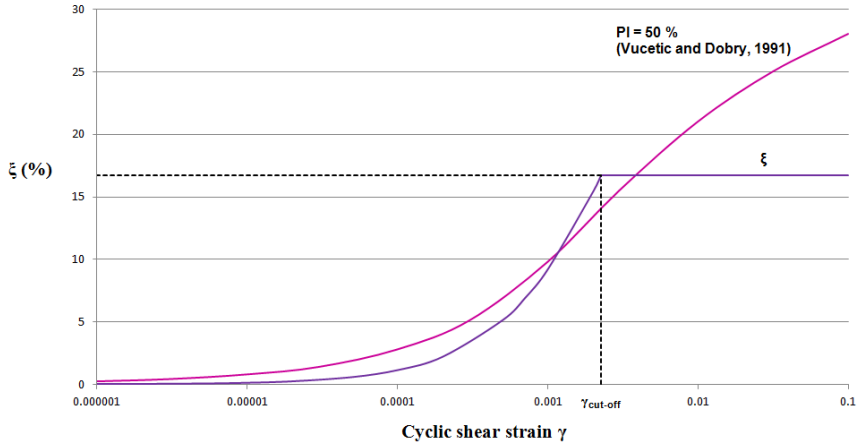


Figure 3.5 Damping curve

The parameters resulting from the calibration are listed in Table 3.1.

| Parameter | Name | Value | Unit |
|---|---|---|---|
| General | | | |
| Material model | Model | User-defined | - |
| Material model | Model | GHS | - |
| Type of material behaviour | Type | Undrained A | - |
| Total unsaturated unit weight of soil | $\gamma_{unsat}$ | 19 | $kN/m^3$ |
| Total saturated unit weight of soil | $\gamma_{sat}$ | 21 | $kN/m^3$ |
| Parameters | | | |
| Secant stiffness in standard drained triaxial test | $E_{50}^{ref}$ | 7680 | $kN/m^2$ |
| Tangent stiffness for primary oedometer loading | $E_{oed}^{ref}$ | 7680 | $kN/m^2$ |
| Unloading / reloading stiffness | $E_{ur}^{ref}$ | 23040 | $kN/m^2$ |
| Power for stress-level dependency of stiffness | $m$ | 0.6 | - |
| Cohesion | $c'_{ref}$ | 30 | $kN/m^2$ |
| Friction angle | $\phi'$ | 26 | ° |
| Dilatancy angle | $\psi$ | 0 | ° |
| Shear strain at which $G_s = 0.722G_0$ | $\gamma_{0.7}$ | 0.0007 | - |
| Shear modulus at very small strains | $G_0^{ref}$ | 48000 | $kN/m^2$ |
| Poisson's ratio | $\nu'_{ur}$ | 0.2 | - |
| Reference stress | $p_{ref}$ | 100 | $kN/m^2$ |
| Failure ratio | $R_f$ | 0.9 | - |
| Tensile strength | $\sigma_t$ | 0 | $kN/m^2$ |
| Overconsolidation Ratio | $OCR$ | 3 | - |
| Pre-overburden pressure | $POP$ | 0 | - |
| Earth pressure coefficient | $k_0$ | 0.973 | - |
| Stress Dependent Stiffness | Stress Dependent Stiffness | 1 | - |
| Strain Dependent Stiffness | Strain Dependent Stiffness | 1 | - |
| Stress Dependency formula | Stress Dependency formula | 0 | - |
| Plasticity model | Plasticity model | 1 | - |

Table 3.1 Material properties of the clay layers (GHS material model)

### 3.2.2 CALIBRATION OF UBC3D-PLM MODEL

The UBC3D-PLM material model is available as a user-defined soil model. For the undrained dynamic calculation the UBC3D-PLM model is used in order to properly model the evolution of the excess pore pressures in the sandy soils and capture the onset of liquefaction. The model parameters are based on $N_{SPT}$ values. Beaty & Byrne (2011) proposed a set of equations based on the normalized $N_{SPT}$ value, $(N_1)_{60}$ for the initial generic calibration of the UBCSAND 904aR model. Makra (2013) revised the proposed equations and highlighted the differences between the UBCSAND 2D formulation and the UBC3D-PLM model, as implemented in PLAXIS. The proposed equations for the generic initial calibration are the following:

$$\phi_p = \phi_{cv} + \frac{(N_1)_{60}}{10} + max\left(0; \frac{(N_1)_{60} - 15}{5}\right) \tag{3.7}$$

$$K_G^e = 21.7 \cdot 20 \cdot (N_1)_{60}^{0.3333} \tag{3.8}$$

$$K_B^e = 0.7 \cdot K_G^e \tag{3.9}$$

$$K_G^p = K_G^e \cdot (N_1)_{60}^2 \cdot 0.003 + 100 \tag{3.10}$$

$$R_f = 1.1 \cdot (N_1)_{60}^{-0.15} \tag{3.11}$$

where $\phi_p$ is the peak friction angle, $\phi_{cv}$ is the friction angle at constant volume, $K_G^e$ is the elastic shear modulus, $K_G^p$ is the plastic shear modulus and $K_B^e$ is the elastic bulk modulus. $R_f$ is the faliure ratio. As for the power for stress dependency of the bulk and shear moduli, $m_e$, $n_e$ and $n_p$, the default values of 0.5, 0.5 and 0.4 respectively, are used. It is suggested to choose a densification factor $fac_{hard}$ of 1.0 and a coefficient of 1.0 for the $fac_{post}$. The friction angle $\phi_{cv}$ has been determined for each layer considering a correlation between the $N_{SPT}$ number and the vertical effective stress. All the 5 sand layers are modeled with UBC3D-PLM in *Undrained A* condition and with $\gamma_{unsat}$ and $\gamma_{sat}$ equal to 14 and 18 $kN/m^3$, respectively.

The set of parameters used for this example can be found in Table 3.2.

To generate the initial stress state correctly, it is necessary to perform the initial phase using another material model with parameters calibrated for the same sand. In this example, the Hardening Soil model has been used (Table 3.3). The total unsaturated and saturated unit weight of soil are equal to 14 and 18 $kN/m^3$, respectively, for all the 5 sand layers. For this calibration, it has been considered that in general $k_G^e \cdot p_{ref}$ is almost equal to the reference value of the initial shear stiffness $G_0^{ref}$ and that the ratio $G_0/G_{ur}$ is about 3. Considering $\nu_{ur}$ equal to 0.2, it is possible to back calculate $E_{ur}$ and $E_{oed}$ and $E_{50}$ as equal to 1/3 of $E_{ur}$. The power coefficient $m$ is usually about 0.5 for sands.

**Hint:** Although we do not use the interfaces, we need to define the interface properties for both user defined soil models. It is suggested to use the same stiffness and strength parameters as the soil material.

| Parameter | Sand layer 1 | Sand layer 2 | Sand layer 3 | Sand layer 4 | Sand layer 5 |
|---|---|---|---|---|---|
| $\phi'_{cv}$ (degrees) | 29.2 | 33 | 29.2 | 32.1 | 32.9 |
| $\phi'_{p}$ (degrees) | 30 | 34 | 30 | 33 | 34 |
| $c'$ $(kN/m^2)$ | 0 | 0 | 0 | 0 | 0 |
| $k_G^e$ | 870.65 | 933.3 | 857 | 917 | 964 |
| $k_G^p$ | 271 | 378 | 253 | 346 | 450 |
| $k_B^e$ | 609.5 | 653 | 600.0 | 642.0 | 675. |
| $me$ | 0.5 | 0.5 | 0.5 | 0.5 | 0.5 |
| $ne$ | 0.5 | 0.5 | 0.5 | 0.5 | 0.5 |
| $np$ | 0.4 | 0.4 | 0.4 | 0.4 | 0.4 |
| $R_f$ | 0.804 | 0.779 | 0.81 | 0.785 | 0.768 |
| $p_{ref}$ $(kN/m^2)$ | 100 | 100 | 100 | 100 | 100 |
| $\sigma_t$ $(kN/m^2)$ | 0 | 0 | 0 | 0 | 0 |
| $fac_{hard}$ | 1.0 | 1.0 | 1.0 | 1.0 | 1.0 |
| $(N_1)_{60}$ | 8.09 | 9.97 | 7.72 | 9.46 | 11 |
| $fac_{post}$ | 1.0 | 1.0 | 1.0 | 1.0 | 1.0 |
| $k_0$ | 0.5 | 0.4408 | 0.5 | 0.4554 | 0.4408 |

Table 3.2 Material properties of the sand layers (UBCSAND material model)

| Parameter | Sand layer 1 | Sand layer 2 | Sand layer 3 | Sand layer 4 | Sand layer 5 |
|---|---|---|---|---|---|
| $E_{50}^{ref}$ $(kN/m^2)$ | 23217 | 24889 | 22857 | 24458 | 25719 |
| $E_{oed}^{ref}$ $(kN/m^2)$ | 23217 | 24889 | 22857 | 24458 | 25719 |
| $E_{ur}^{ref}$ $(kN/m^2)$ | 69652 | 74667 | 68571 | 73373 | 77156 |
| $m$ | 0.5 | 0.5 | 0.5 | 0.5 | 0.5 |
| $c'$ $(kN/m^2)$ | 0 | 0 | 0 | 0 | 0 |
| $\phi$ (°) | 30 | 34 | 30 | 33 | 34 |
| $\psi$ (°) | 1 | 1 | 1 | 1 | 1 |
| $k_0$ | 0.5 | 0.4408 | 0.5 | 0.4554 | 0.4408 |

Table 3.3 Material properties of the sand layer (Hardening Soil model)

### 3.2.3 CALIBRATION OF RAYLEIGH DAMPING COEFFICIENTS

Hysteretic damping of the soil model can capture damping at strains larger than $10^{-4}$ - $10^{-2}$ %, depending on the values of material properties. Even at low deformation levels, the behaviour of the soil is irreversible. It is suggested to define the Rayleigh damping coefficients associated to a small damping ratio for all clay and sand layers. According to the Rayleigh damping formulation, the damping matrix C is given by a portion of the mass matrix M and a portion of the stiffness matrix K, as a function of the Rayleigh coefficients

$\alpha$ and $\beta$:

$$[C] = \alpha[M] + \beta[K] \tag{3.12}$$

In the *General* tabsheet of the created material, by clicking on the *Rayleigh* $\alpha$ box, the window expands on the right side and it is possible to calculate the Rayleigh coefficients by entering proper values for the damping ratios and the target frequencies (Figure 3.6).

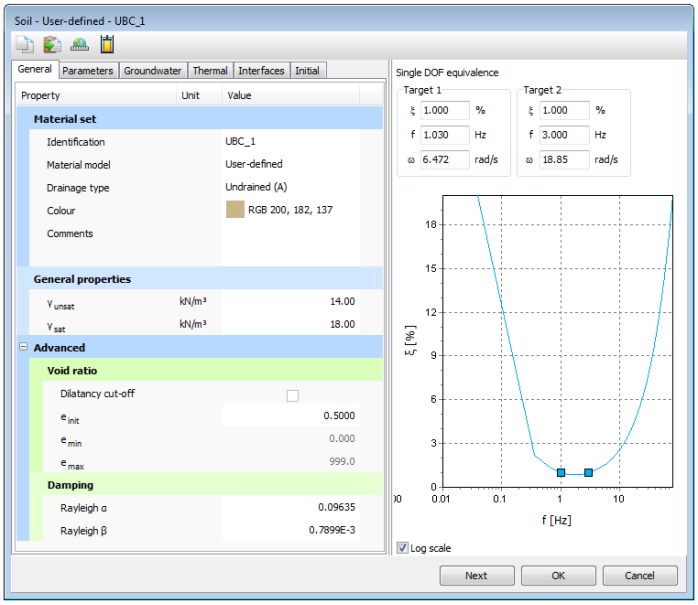


Figure 3.6 Rayleigh damping coefficients.

To calibrate these two coefficients, it is necessary to define the target damping ratios $\xi$ and the related frequencies. It is suggested to keep the same value of $\xi$ for both Target 1 and 2, generally chosen between 0.5 and 2 %. Several strategies can be found in literature to select the appropriate frequencies. Hudson, Idriss & Beirkae (1994) proposed to set the first frequency equal to the fundamental frequency of the whole soil layer, and the second frequency as the closest odd number given by the ratio of the fundamental frequency of the input signal at the bedrock and the fundamental frequency of the whole soil layer. The fundamental frequency of the soil deposit is defined as the frequency at which the most significant amplification can be expected, and it corresponds to the first mode shape. According to this procedure, the frequency of Target 1 is given by:

$$f = \frac{v_s}{4H} \tag{3.13}$$

where $v_s$ represents the shear wave velocity and H is the thickness of the soil layer. The value of $v_s$ has been chosen as an average value over the whole depth. Based on the shear stiffness profile $G_0$ and the unit weight of soil $\gamma$, it is possible to calculate the shear wave velocity profile with depth:

$$v_s = \sqrt{\frac{G}{\rho}} \tag{3.14}$$

where $\rho$ is equal to the ratio of $\gamma$ over the gravity acceleration $g$.

Considering that the average value of $v_s$ is about 166 $m/s^2$ and the soil deposit is 40 m thick, the fundamental frequency is equal to 1.03 Hz. Considering the Fourier spectrum of the input signal at the bedrock, it can be found that the fundamental frequency of the signal is 2.465 Hz which gives a ratio 2.46/1.03 equal to 2.4 Hz. Therefore, the frequency of Target 2 is set equal to 3 Hz. Within the range of the chosen frequencies the damping is less than the target damping, whereas outside this range the signal is overdamped. Using a target damping ratio of 1 %, the values of the Rayleigh coefficient $\alpha$ and $\beta$ are 0.09635 and 0.0007899, respectively.

### 3.2.4 CALIBRATION OF THE LINEAR ELASTIC MATERIAL

The rock formation at the basis of the model has to be modeled through a linear elastic material model with drained condition. Usually, shear wave velocity higher than 800 m/s indicates a rock-like formation. According to the specified values, the corresponding wave velocity is equal to 1220 m/s.

The parameters in Table 3.4 have been used.

| Parameter | Name | Value | Unit |
|---|---|---|---|
| General | | | |
| Material model | Model | Linear Elastic | - |
| Type of material behaviour | Type | Drained | - |
| Total unsaturated unit weight of soil | $\gamma_{unsat}$ | 22 | $kN/m^3$ |
| Total saturated unit weight of soil | $\gamma_{sat}$ | 22 | $kN/m^3$ |
| Parameters | | | |
| Elastic modulus | $E$ | 8011000 | $kN/m^2$ |
| Poisson's ratio | $\nu'_{ur}$ | 0.2 | - |

Table 3.4 Material properties of the rock formation (LE material model)

## 3.3 DEFINITION OF THE LOADING CONDITION

The ground motion input used in this example corresponds to the accelerogram characterized by a moment magnitude $M_w$ equal to 6.9. The input signal is scaled at a peak horizontal acceleration of 0.3 g. The earthquake is assumed to be given at the outcrop of a rock formation and is modelled by imposing a prescribed displacement at the bottom boundary. Considering that the boundary condition at the base of the model will be defined using a compliant base, the input signal has to be taken as half of the outcropping motion. By definition, the time history acceleration that is needed as input to the compliant base is the upward motion. The outcrop motion is characterized by the upward and downward motions, which have the same wave amplitude.

PLAXIS allows to specify the input motion as a prescribed displacement along the base of the model. For this example, considering that half of the input motion is needed, a value of 0.5 m has to be assigned to the x-component of the prescribed displacement, while the y-direction is fixed. The dynamic load is given in terms of dynamic multiplier by

importing the input signal and selecting the *Acceleration* option. The dynamic load is given in $m/s^2$ and has a peak of 3 $m/s^2$. The file containing the earthquake data is available in the PLAXIS knowledge base and can be saved on your personal computer (http://kb.plaxis.nl/search/site/amax=3_amax=0_3g).

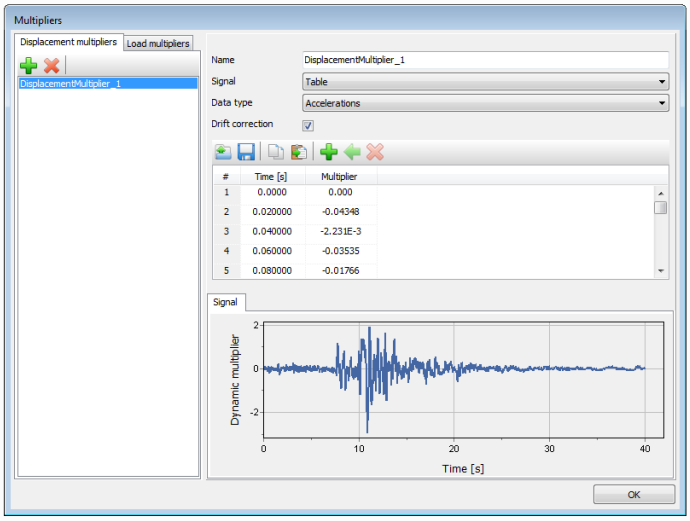


Figure 3.7 Dynamic multiplier

By selecting the drift correction option, PLAXIS corrects the possible drift in the displacements (i.e. non null final displacement in the signal), caused by the integration of the accelerations and velocities. The correction is made by applying a low frequency motion from the beginning of the phase of the calculation and by correcting the acceleration accordingly. For a correct drift correction, the time interval of the phase and of the input signal should be the same. In order to model a compliant base, it is required to specify an interface at the bottom of the model.

## 3.4 MESH GENERATION

The mesh generation is fully automatic and based on a robust triangulation procedure. The dimension of the triangular elements needs to be controlled and the mesh refinement allows to get a specific value for the average length of the element side. Kuhlemeyer & Lysmer (1973) suggest to assume a size less than or equal to one-eight of the wavelength associated with the maximum frequency component $f_{max}$ of the input wave (i.e. the highest frequency component that contains appreciable energy):

$$AverageElementSize \leq \frac{\lambda}{8} = \frac{v_{s,min}}{8 f_{max}} \tag{3.15}$$

where $v_{s,min}$ is the lowest wave velocity. Based on the shear stiffness profile and the unit weight of soil, it is possible to calculate the shear wave velocity profile with depth. The lowest $v_s$ is equal to 113 $m/s$. From the Fourier spectrum it can be found that the maximum frequency component is about 5 Hz, which leads to an average length of 2.8 m (Eq. (3.15)).

The horizontal dimension of the model has been chosen equal to 2.5 m.

## 3.5 DEFINITION OF THE BOUNDARY CONDITIONS AND OF THE CALCULATION PARAMETERS

The boundary conditions may be chosen in the *Staged construction* mode. The calculation process consists of the initial conditions phase, a nil-step that allows to generate correctly the initial stress in the case of user-defined soil models and the free-field seismic analysis for triggering liquefaction. The first two phases are static and default fixities can be applied, corresponding to normally fixed vertical boundaries and a fully fixed base. The third phase is dynamic. In the *Model explorer* the prescribed displacement and its dynamic component have to be activated. The vertical boundaries are modeled with tied degrees of freedom, while the compliant base option can be selected at the base ($Y_{Min}$). In order to properly apply these boundary conditions, an interface at the bottom of the model has to be introduced but not activated and the static fixities has to be deselected.

There are several possibilities to model the boundary conditions for a dynamic analysis. For the lateral boundaries, in the case of a one-dimensional wave propagation, the option Tied degrees of freedom allows to model a reduced geometry of the problem. It is sufficient to define a soil column with the horizontal dimension defined according to the average element size, while the nodes at the left and right model boundaries are connected to each other and are characterized by the same displacement. The *Tied degrees of freedom* boundary conditions can only be applied if the distribution of nodes along the two vertical model boundaries is identical, i.e the corresponding nodes at the left and right side should have the same y-coordinate. In PLAXIS 2D2015, these boundary conditions only work on boundaries that are free to move. For this reason it is required to switch off the default fixities.

As for the base of the model, the most common case is that of a soil deposit with non linear behaviour overlying a bedrock, assumed to behave linearly and to be able to absorb the downward propagating waves. To model this condition a compliant base has to be specified at the bottom of the model. A compliant base is based on the same principles of the free field boundaries, where free field elements are added to the main domain and are connected to it by means of dashpots attached in the normal and shear directions. To describe the propagation of wave inside the element, the same mechanical behaviour of the surrounding soil is used. The motion of the element is transferred to the main domain by applying the equivalent forces, which are automatically calculated by PLAXIS. Considering only the shear direction, the shear stress is given by:

$$\tau = 2 \cdot \rho \, C_2 \, v_s \, \dot{u}_{upward} \tag{3.16}$$

where $\rho$ is the density of the material, $C_2$ is a relaxation coefficient, $v_s$ is the shear wave velocity in the element and $\dot{u}_{upward}$ is the particle velocity of the upward propagation motion. The factor 2 is added since half of the stress is absorbed by the viscous dashpots and half is transferred to the main domain. It has to be noted that only the upward motion is needed: if the earthquake is recorded at the outcrop of a rock formation it consists of the superposition of the upward and downward propagating waves, i.e. half of the motion should be used as input to the analysis (since the upward and downward waves amplitudes are the same). The compliant base work properly if the relaxation coefficient

$C_2$ is equal to 1. The values of $\rho$ and $v_s$ are the ones of the soil layer at the base. This means that, if the input motion is recorded at the outcrop of a rock-like formation with high shear wave velocity and elastic properties, it is required to define a thin layer at the base of the model with the properties of a rock. To model a compliant base in PLAXIS, it is not necessary to define a stress-time history but the user can apply a prescribed displacement and give the input in terms of time-acceleration, velocity or displacement. The separation between the main domain and the free field element at the base is done by means of an interface, which allows for the creation of a so called node pair: in this way it is possible to both apply the input motion and absorb the incoming waves.

The calculation parameters of the dynamic phase have to be properly specified in the *Phases* window, by selecting:

- Set the *Dynamic* option as *Calculation* type
- Set 40 s as the *Dynamic time interval*
- Set the *Maximum number of steps* equal to 2000 and keep the default settings for the other numerical control parameters
- Keep the default values for *Alpha-Newmark* and *Beta-Newmark* (0.25 and 0.5, respectively).

The automatic procedure implemented in PLAXIS ensures that a wave does not cross more than one element per time step. The conditions to be verified are two: at first, the critical time step is estimated according to the element size and the material stiffness, then the time step is adjusted based on the number of data points specified as dynamic multipliers.

The time step $\delta t$ used in a *Dynamic calculation* is given by:

$$\delta t = \frac{\Delta t}{m \cdot n} \tag{3.17}$$

where $\Delta t$ is the *Dynamic time interval* parameter, i.e. the duration of the earthquake, $m$ is the *Max steps number* and $n$ is the *Number of sub steps*. PLAXIS automatically calculates the proper number of steps $n$ and sub steps $m$. In order to visualize the complete signal, it is advised to use a number of steps $m$ equal to the number of multipliers that defines the input signal.

To visualize the values calculated by PLAXIS, the user can select *Manual* in the *Time step determination* menu. The *Number of sub steps* box becomes editable and, by clicking that box, a table appears, where the user can press the *Retrieve* button and calculate the number of sub steps needed. Click *Apply* to use the displayed values in the calculation. By modifying the calculated values and using a time step that is larger than the specified limits, the data are interpolated and this may lead to inaccurate results. To check if the used signal is the same as the one given in input, it is possible to create a chart in the *Output* program selecting *Dynamic time* on the X-axis and $a_x(g)$ on the Y-axis at the bottom level. The signal given in this chart should be the same as the input signal.

**Hint:** Before starting the calculation, it is advised to select nodes and stress points at the depth of interest.

### 3.6 RESULTS

The liquefaction potential can be expressed by means of the excess pore pressure ratio $r_u$, which represents the ratio of the excess pore pressure and the initial effective vertical stress at that depth. For the UBC3D-PLM model, $r_u$ is given by:

$$r_u = 1 - \frac{\sigma'_v}{\sigma'_{v0}} \tag{3.18}$$

where $\sigma'_v$ is the vertical effective stress at the end of the dynamic calculation and $\sigma'_{v0}$ is the initial effective vertical stress prior to the seismic motion. When $r_u$ is equal to 1, the corresponding layer is in a complete liquefied state. Beaty and Perlea (2011) consider zones with a maximum $r_u$ greater than 0.7 to be liquefied. Figure 3.8 shows that liquefaction occurs in all the five sand layers, since the $r_u$ parameter is about 1 at the end of the analysis.

The values of the excess pore pressures in those layers are very high (Figure 3.9a) and consequently, the effective stresses are almost zero (Figure 3.9b).

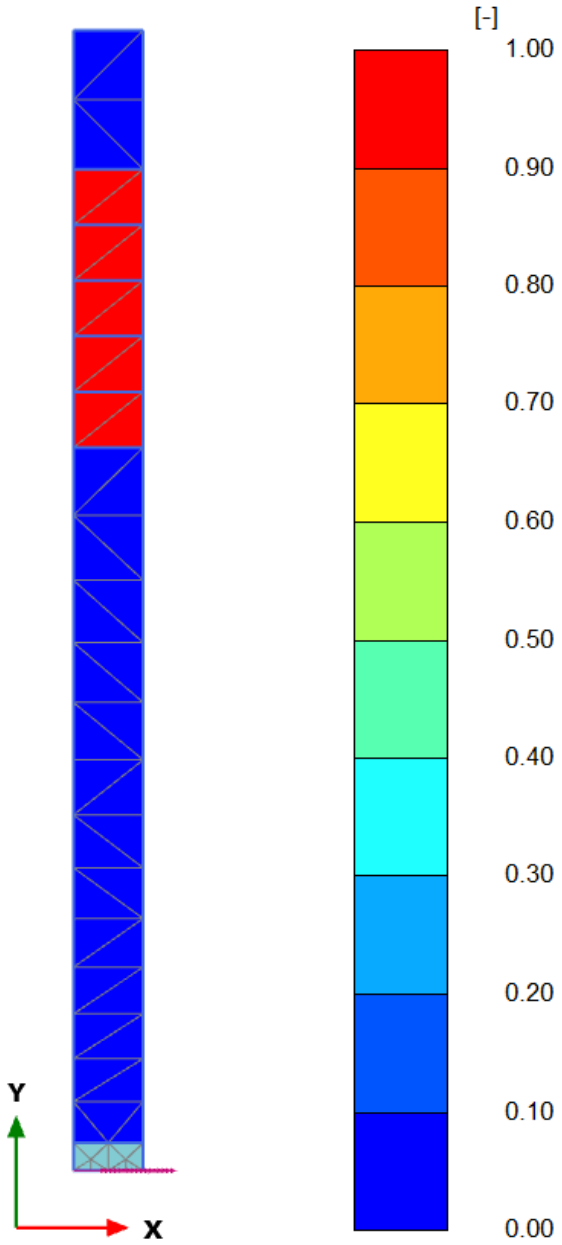


Figure 3.8 Pore pressure ratio.

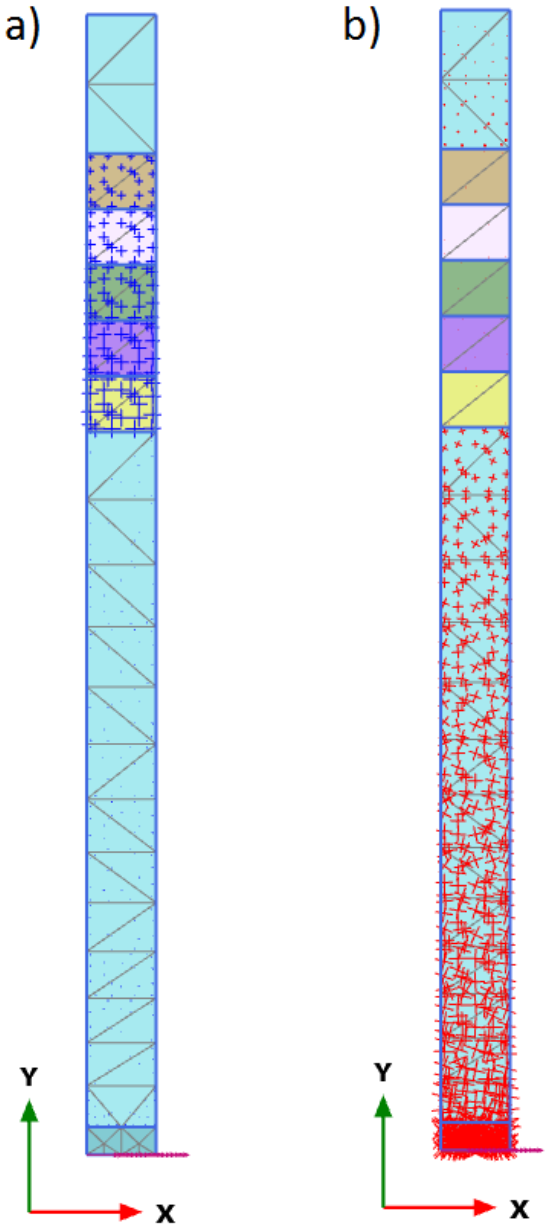


Figure 3.9 Excess pore pressure (a) and effective stresses (b).

### 3.7 CONCLUSIONS

This example presents the results of a dynamic analysis performed with the PLAXIS finite element code, aimed at modelling the onset of liquefaction in loose cohesionless soils. Two different approaches, commonly used in engineering practice, are compared. First, the simplified procedure introduced by Seed & Idriss (1971) and updated by Idriss & Boulanger (2014) is carried out. The onset of liquefaction is determined by a curve which separates a liquefiable state from a non liquefiable state. This curve is built on the basis of a large number of case-histories. This approach is based on a series of coefficients that allow to "scale" the seismic event and the in situ conditions to a standard situation. The second approach consists of a fully dynamic analysis by means of the finite element code PLAXIS 2D. In this case, it is important to select the appropriate dynamic boundary conditions and constitutive models to reproduce the behaviour of saturated soils under cyclic loads. The results of the PLAXIS calculation are in good agreement with the results of the simplified procedure, since the onset of liquefaction is successfully modelled in all the five sand layers.

As for the constitutive models, the UBC3D-PLM model can be considered capable of modelling the accumulation of excess pore pressures in saturated loose sands subjected to cyclic loading, while the GHS model is able to reproduce the non-linear dissipative behaviour of soils during cyclic shear loading, by activating only the failure surface. This research has shown that the GHS model can be used to describe the stiffness degradation and an appropriate damping curve by means of a non linear elastic behaviour until failure is reached, avoiding that the plastic deformations developed when reaching the cap and hardening surfaces lead to an overdamping of the earthquake characteristics. Previous works have shown some limitations in the UBC3D-PLM model, which is not appropriate to generate the initial stresses during gravity loading and it is associated to an overdamping due to the use of $G_{max}$ in elastic unloading. To overcome the problems with the generation of initial stresses, it suggested to assign one of the materials which are available in the library (such as Hardening Soil model as shown in the document) during the *Initial phase*, and then substitute the material with UBC3D-PLM for the following phases.

As for the boundary conditions, the tied degrees of freedom option allows to successfully model a reduced geometry for a 1D wave propagation analysis, while the bottom boundary can be modeled as a compliant base by applying a prescribed displacement, without any conversion to a distributed load.

## 4 REFERENCES

[1] Beaty, M.H., Byrne, P.M. (2011). Ubcsand constitutive model. Itasca UDM website 904aR.

[2] Beaty, M.H., Perlea, V.G. (2011). Several observations on advanced analyses with liquefiable materials. Thirty first annual USSD conference on 21st century dam design-advances and adaptations, 1369–1397.

[3] Benz, T. (2007). Small-strain stiffness of soil and its numerical consequences. PhD Thesis, Institute of Geotechnical Engineering, University of Stuttgart.

[4] Boulanger, R.W., Kutter, B.L., Brandenberg, S.J., Singh, P., Chang, D. (2003). Pile foundations in liquefied and laterally spreading ground during earthquakes:centrifuge experiments & analyses.

[5] Galavi, V., Petalas, A., Brinkgreve, R.B.J. (2013). Finite element modelling of seismic liquefaction in soils. Geotechnical engineering journal of Ihe SEAGS and AGSSEA, 44 (3): 55–64.

[6] Hudson, M., Idriss, I., Beirkae, M. (1994). Quad4m user's manual.

[7] Idriss, I.M. (1990). Response of soft soil sites during earthquakes. H Bolton Seed Memorial Symposium, 2: 273–290.

[8] Idriss, I.M. (1991). Earthquake ground motions at soft soils. 2nd International conference on Recent adv. in Geotech. Earthquake Engg and Soil Dyn., 3: 2265–2271.

[9] Idriss, I.M. (1999). An update to the seed-idriss simplified procedure for evaluating liquefaction potential. Proceedings, TRB Workshop on New Approaches to Liquefaction, FHWARD–99–165.

[10] Idriss, I.M., Boulanger, R.W. (2004). Semi-empirical procedures for evaluating liquefaction potential during earthquakes. Proceedings, 11th International Conference on Soil Dynamics and Earthquake Engineering, and 3rd International Conference on Earthquake Geotechnical Engineering, D. Doolin et al., eds., Stallion Press, 1: 32–56.

[11] Idriss, I.M., Boulanger, R.W. (2008). Soil liquefaction during earthquakes. Monograph MNO-12, Earthquake engineering research institute, Oakland.

[12] Idriss, I.M., Boulanger, R.W. (2010). Spt-based liquefaction triggering procedures. Report UCD/CGM - 10/02, Department of civil and environmental engineering, University of California.

[13] Idriss, I.M., Boulanger, R.W. (2014). Cpt and spt based liquefaction triggering procedures. Report UCD/CGM-14/01, Department of civil and environmental engineering, University of California.

[14] Kuhlemeyer, R.L., Lysmer, J. (1973). Finite element method accuracy for wave propagation problems. Journal of soil mechanics and foundation devision, 99 (5): 421–427.

[15] Liao, S., Whitman, R.V. (1986). Overburden correction factors for spt in sand. Journal of Geotecnical Engineering ASCE 112(3), 373–377.

[16] Makra, A. (2013). Evaluation of the ubc3d-plm constitutive model for prediction of earthquake induced liquefaction on embankment dams.

[17] Petalas, A., Galavi, V. (2013). Plaxis liquefaction model ubc3d-plm. PLAXIS knowledge base.

[18] Schanz, T., Vermeer, P.A., Bonnier, P.G. (1999). The hardening soil model: formulation and verification. Beyond 2000 in Computational Geomechanics, 281–296.

[19] Seed, H.B., Idriss, I.M. (1967). Analysis of liquefaction: Niigata earthquake. Proceedings ASCE, 93 (SM3), 83–108.

[20] Seed, H.B., Idriss, I.M. (1971). Simplified procedure for evaluating soil liquefaction potential. Journal of the Soil Mechanics and Foundations Division 97 (9), 1249–1273.

[21] Seed, R.B., Dickenson, S.E., Rau, G.A., White, R.K., Mok, C.M. (1994). Site effects on strong shaking and seismic risk: Recent developments and their impact on seismic design codes and practice. Struct. Congr II, 1: 573–578.

[22] Tsegaye, A. (2010). Plaxis liquefaction model. external report. PLAXIS knowledge base.

[23] Vucetic, M., Dorby, R. (1991). Effect of soil plasticity on cyclic responses. Journal of geotechnical engineering, ASCE 117(GT1), 89–107.

[24] Youd, T.L., Idriss, I.M., Andrus, R.D., Arango, I., Castro, G., Christian, J.T., Dobry, R., Finn, W.D.L., Jr, L.F.H., Hynes, M.E., Ishihara, K., Koester, J.P., Liao, S.S.C., III, W.F.M., Martin, G.R., Mitchell, J.K., Moriwaki, Y., Power, M.S., Robertson, P.K., Seed, R.B., II, K.H.S. (2001). Liquefaction resistance of soils: Summary report from the 1996 nceer and 1998 nceer/nsf workshop on evaluation of liquefaction resistance of soils. Journal of Geotechnical and Geoenvironmental engineering, 817–833.